Chinese Chemical Letters 32 (2021) 3837–3840

Contents lists available at ScienceDirect

Chinese Chemical Letters

journal homepage: www.elsevier.com/locate/cclet

Communication

A hexaazatriphenylene fused large discotic polycyclic aromatic hydrocarbon with selective and sensitive metal-ion sensing properties

Wenxiu Qu, Wei Yuan, Mengwei Li, Yulan Chen*

Tianjin Key Laboratory of Molecular Optoelectronic Sciences, Department of Chemistry, Institute of Molecular Plus, Tianjin University, Tianjin 300072, China

ARTICLE INFO

Article history:
Received 26 March 2021
Revised 14 May 2021
Accepted 20 May 2021
Available online 26 May 2021

Keywords:
Hexaazatriphenylene
Ion adsorption
Ion sensing
Polycyclic aromatic hydrocarbons
Self-assembly

ABSTRACT

A HAT based large PAH discotic molecule PN_8 is developed. The enlarged chromophoric core and doping heteroatoms enable colorimetric and fluorometric sensing of Cu^{2+} and Zn^{2+} with highly appreciable optical changes, good selectivity and low detection limit. Moreover, PN_8 was demonstrated as an excellent adsorbent to remove Cu^{2+} and Zn^{2+} from wastewater.

Discotic polycyclic aromatic hydrocarbons (PAHs) have been of great interest in materials science and nanoscience [1]. Due to the structure tailorability, self-assembled ability and the appealing optical and electronical features of disc PAHs [2–8], they are ideal candidates for smart matters with diverse applications [9,10]. For instance, up to now, different disc-PAHs have been designed and synthesized with the aim of using them for molecular recognition and fluorescent sensors [11,12]. In this context, extending chromophoric group and doping heteroatoms are two practical strategies to improve the sensitivity and selectivity of the respective sensors, since the fluorescence intensity, energy level and intermolecular interactions could be fine-tuned.

1,4,5,8,9,12-Hexaazatriphenylene (HAT, Fig. 1) represents the smallest two-dimensional *N*-containing PAH. The doped N atoms offer three chelating sites to the metal ions, so that the HAT derivatives have been widely used in fluorescent chemosensors and metal-containing supramolecular materials [13–15]. In most cases, HAT derivatives possess low fluorescence quantum yields partially due to the forbidden S_0–S_1 transition [1,16]. Or, their absorption and emission colors are usually located in the violet and blue light region which are not sensitive to naked eyes [16,17]. In this regard, more knowledge and examples about the improved sensitivity of the HAT based chemical sensors consisting of enhancing the fluorescence intensity and tuning the emission color are welcome.

Recently, we reported a type of S,N-doped disc PAHs based on a π-extended, thiophene-fused phenanthroline unit (S,N-PAH, Fig. 1). The large conjugated mesogenic core with increased dipole moment derived from S,N heteroatoms not only facilitates the formation of highly ordered columnar superstructures, but also endows distinct bathochromic shifts of absorption and emission maxima compared to the smaller dibenzo[*a,c*]phenazine counterpart [18,19]. Despite their excellent optical properties, their ion sensing feature was not observed, mainly due to the lack of efficient chelating sites. Based on our continuous interests in the synthesis and functions of large disc PAHs, in this work, we designed and explored a novel disc PAHs molecule with a unique metal-ion sensing character, by fusion the phenanthroline unit with a HAT moiety (PN_8, Fig. 1). With two phenyl groups fused at the nitrogen-containing heterocycles, the core size of PN_8 is larger than the reported S,N-PAH [19], with an expectation to the bathochromic shift of fluorescence colors, as well as the increase of overall dipole moment and anisotropic self-assembly ability. We also envisioned that the incorporated N heteroatoms in the aromatic core would provide more coordination sites, which may give rise to the recognition of metal ions for optical sensing applications. Consequently, PN_8 exhibited a great tendency to self-assemble into long-range ordered aggregates. Moreover, both the self-assembled microfibers and the solutions were sensitively responsive to Cu^{2+} or Zn^{2+}, accompanied by either quenched fluorescence or redshift emission colors. Meanwhile, the two metal ions could trigger dis-assembly of the microfibers. The efficient chelating ability of this newly emerged PAH molecule allowed its application as an adsorbent for the removal of Cu^{2+} and Zn^{2+} from wastewater.

* Corresponding author.
E-mail address: yulan.chen@tju.edu.cn (Y. Chen).

https://doi.org/10.1016/j.cclet.2021.05.044
1001-8417/

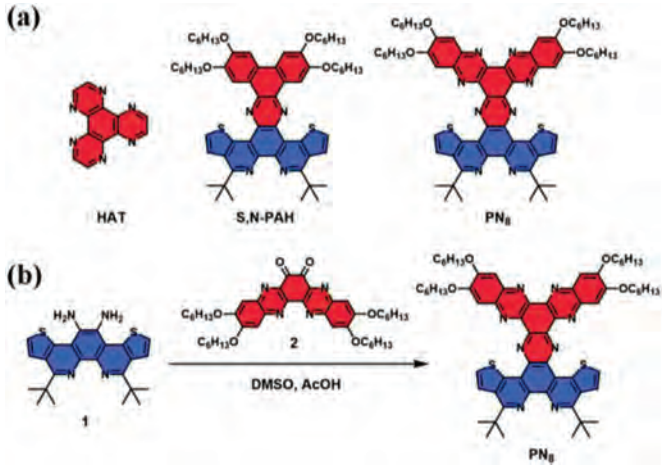

Fig. 1. (a) Chemical structures of HAT, S,N-PAH and PN_8. (b) Synthetic route of the target molecule PN_8.

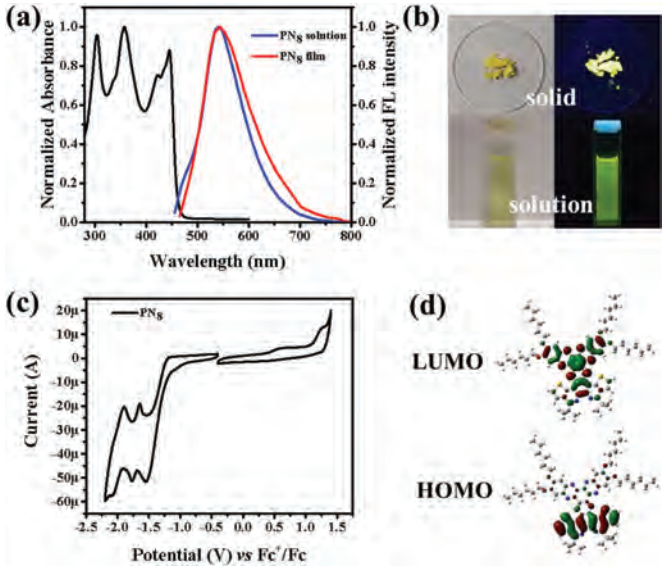

Fig. 2. (a) UV–vis absorption and fluorescence emission spectra of PN_8 in chloroform (1×10^{-5} mol/L, λ_{ex} = 445 nm) and in solid state. (b) The corresponding photographs under visible light (left) and 365 nm UV light (right). (c) Cyclic voltammograms of PN_8 measured in dichloromethane with 0.1 mol/L $TBAPF_6$ as electrolyte (scan rate = 100 mV/s). (d) DFT calculated molecular-orbital amplitude plots and energy levels for PN_8 in the gas phase.

The structure and synthetic route of the target molecule PN_8 are presented in Fig. 1 and Scheme S1 (Supporting information). PN_8 is an asymmetric π-extended HAT disc molecule surrounded by hexyloxy chains, which can be synthesized straightforwardly, by condensation of the thiophene-fused phenanthroline-11,12-diamine **1** with quinoxalino[2,3-*a*]-phenazine-6,7–dione **2** in the presence of acetic acid in a yield of 26%. The target compound PN_8 was unambiguously characterized by NMR spectroscopy (^1H and ^{13}C) and mass spectrometry (Figs. S9-S11 in Supporting information). The proton peaks of PN_8 have been assigned explicitly in Fig. S9. And HR-ESI-MS spectrum of PN_8 revealed a single species (*m/z*: 1111.5660 for $C_{66}H_{78}N_8O_4S_2H$ $[M + H]^+$) in accordance with the calculated value.

In dilute chloroform solution, PN_8 showed intense UV-vis absorption ranging from 250 nm to 500 nm with four distinct bands centered at 303 nm ($\varepsilon = 9.75 \times 10^4$ L mol^{-1} cm^{-1}), 357 nm ($\varepsilon = 10.25 \times 10^4$ L mol^{-1} cm^{-1}), 417 nm ($\varepsilon = 7.55 \times 10^4$ L mol^{-1} cm^{-1}) and 445 nm ($\varepsilon = 8.75 \times 10^4$ L mol^{-1} cm^{-1}), assignable to the π-π^* and n-π^* transitions of the PAH core (Fig. 2a). PN_8 displayed bright fluorescence emission in the green-yellow region at 500–750 nm with a maximum emission at approximately 540 nm. In solid state, PN_8 exhibited bright yellow fluorescence with the absolute quantum yield rising from 2.32% in chloroform solution to 7.66%, suggesting the aggregation-enhanced emission (AEE) property [20] (Fig. 2b). Compared to many reported HAT derivatives, there are distinct bathochromic shifts of the absorption and emission colors, owing to the extended conjugation of the chromophore core [21].

The electrochemical properties of PN_8 were studied both experimentally and theoretically. First, the cyclic voltammograms of PN_8 in dichloromethane are shown in Fig. 2c. Different from S,N-PAH that only exhibited one reversible reduction peak, three reduction waves at −1.55, −1.77 and −2.09 V for PN_8 were observed, which were attributed to the consecutive reduction steps of three pyrazine moieties [22]. The onset of the first oxidation (E_{ox}) and reduction onset (E_{red}) was 0.37 eV and −1.17 eV, respectively. The corresponding ionization potentials (IP) and electron affinities (EA) energy levels were thus estimated to be 5.03 and 3.53 eV, respectively. Compared to S,N-PAH, the reduced EA energy level for PN_8 was ascribed to the electron-deficient nature of the fused HAT part. On the other hand, according to DFT calculation results, the calculated PN_8 adopted a highly planar configuration, with the LUMO electrons delocalized over the HAT moiety, whereas the HOMO electrons unevenly distributed over the thiophene-fused 1,10-phenanthroline part (Fig. 2d). It is noteworthy that the calculated dipole moment of PN_8 is larger than that of S,N-PAH, possibly due to the joint effects from the π-expanded core and more doped nitrogen atoms (Table S1 in Supporting information).

As a large conjugated disc molecule with a strong local dipole, PN_8 was readily to self-assemble into anisotropic superstructures. The self-assembled behavior of PN_8 was first examined by concentration-dependent ^1H NMR spectra. As shown in Fig. S1 (Supporting information), all the aromatic signals shifted upfield and became less-resolved with the concentration increasing. This indicated that PN_8 formed stacked assemblies in which the aromatic protons were placed in the shielding regions produced by the neighboring aromatic rings. The peak assigned for $-OCH_2$ protons also became broad and non-splitting at high concentration, implying that the alkyl chains were also involved in the assembly process [23]. Morphological study based on scanning electron microscopy (SEM) technique also confirmed the formation of microfibrils with high aspect ratios. For instance, in THF or mixed solutions, either three-dimensional networks composed of interdigitated long and rigid microfibers (in chloroform/acetone), or flexible high aspect ratio microwires (in chloroform/methylcyclohexane) were observed, with the widths in the range of 100–400 nm and the lengths up to tens of micrometers (Fig. S2 in Supporting information). Interestingly, these well-ordered 1D assemblies could experience reversibly morphological transitions upon alternate treatment with metal ions and EDTA solution. As shown in Fig. 3a, when Cu^{2+} or Zn^{2+} was added to the PN_8 suspension, the initially formed fiber structures quickly crashed, resulting in ill-defined nanoaggregates. And the regular 1D assemblies could be re-generated when the resulted solution was treated with EDTA. Accompanied with morphological changes, appreciable color changes of the suspension and solutions could be easily detected by naked eyes (Fig. 3b). Such transition cycle can be repeated many times without the chemical decomposition of PN_8, indicating the existence of supramolecular interactions between PN_8 and metal ions.

These results inspired us to further explore the ion-sensing properties of PN_8. Its responsive behaviors in dilute solution were

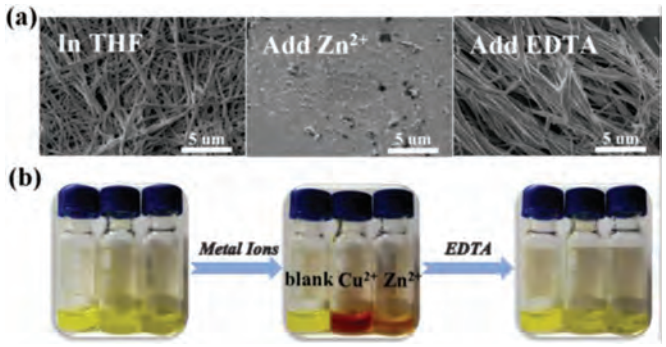

Fig. 3. (a) SEM images of assembled PN_8 from THF (left), then treated with Zn^{2+} (middle), followed by treatment with EDTA (right) and (b) the corresponding photographs.

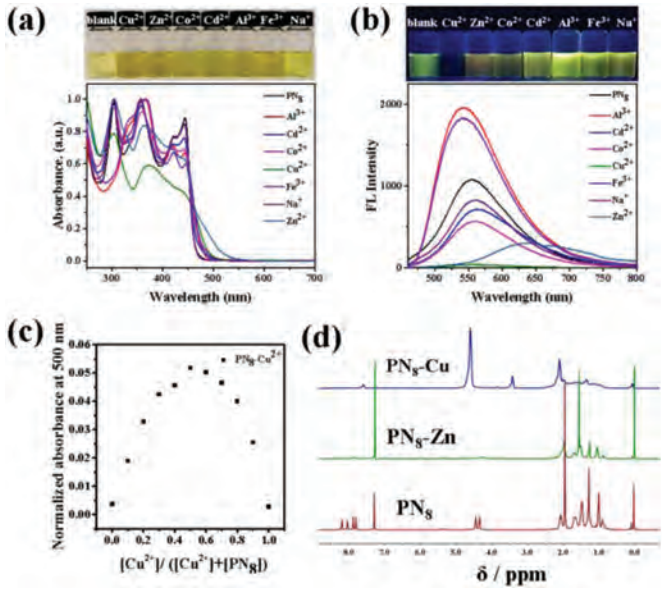

Fig. 4. (a) UV-vis absorption and (b) fluorescence spectra of PN_8 in chloroform (1×10^{-5} mol/L, λ_{ex} = 445 nm) with addition of different metal ions (4 equiv.), and the corresponding photographs under visible light and 365 nm UV light. (c) Job plot for the PN_8-Cu^{2+} system. $[PN_8]+[Cu^{2+}]$ = 0.1 mmol/L. (d) ^1H NMR spectra of PN_8 and PN_8 with 4 equiv. metal ions in $CDCl_3$.

screened by adding different cations, like Al^{3+}, Cd^{2+}, Co^{2+}, Cu^{2+}, Fe^{3+}, Na^+ and Zn^{2+}. PN_8 was found selectively responsive to Cu^{2+} and Zn^{2+}. In detail, the addition of Cu^{2+} and Zn^{2+} led to the red-shift of absorption onset, so the color of the solution became deep yellow (Fig 4a). More remarkably, according to FL spectra (Fig. 4b), Cu^{2+} caused almost complete fluorescence quenching, while for Zn^{2+}, not only the decreased fluorescence intensity, but also a distinct red-shift emission color was detected for its mixed solution. The emission maximum varied from 547 nm to 630 nm after the treatment of Zn^{2+}. Under the same conditions, an increase of emission intensity was observed after Al^{3+} or Fe^{3+} was added; while a slight decrease after treated with other ions. The enhanced emission might be due to the Lewis acidity of Al^{3+} and Fe^{3+}, as a similar phenomenon appeared after TFA was added to the PN_8 solution (Fig. S3 in Supporting information). In contrast to Cu^{2+} and Zn^{2+}, such fluorescence change of the solution upon treated with the other tested metal ions was not readily discriminated by naked eyes, therefore, PN_8 is promising to serve as a fluorescent optical probe for metal ions, such as Cu^{2+} and Zn^{2+}.

Following, the detection limit was evaluated on the basis of fluorescence titration experiments [24]. The plot of fluorescence intensity of the PN_8 (1×10^{-5} mol/L) *vs.* concentrations of Cu^{2+} in $CHCl_3$ displayed a good linear relationship with R^2 of 0.9878 during titration. The limit of detection (LOD) for Cu^{2+} was determined to be 8.71×10^{-7} mol/L for PN_8 (Fig. S4 in Supporting information) based on LOD = $3\sigma/k$, where σ is the standard deviation of blank measurements and k is the slope. Meanwhile, the fluorescence wavelength of the solutions showed a good linear relationship (R^2 = 0.9954) with the concentration of Zn^{2+}, with LOD for Zn^{2+} determined to be 8.57×10^{-8} mol/L. Both values are comparable to many reported ones [15, 25–27].

To shed more light on the ion-sensing mechanism, a set of experiments were carried out. First, no optical changes were detected after the acidification of PN_8 solution, therefore, the responsive properties of PN_8 towards Cu^{2+} and Zn^{2+} presumably derived from pH variation or protonation could be excluded. Also, the control compounds S,N-PAH and the thiophene-fused phenanthroline part alone TP were found not responsive to metal ions (Fig. S5 in Supporting information). Based on these facts and combined with the molecular structure, we inferred a binding mechanism mainly arisen from the fused HAT unit. Although attempts to obtain single crystals of PN_8 with Cu^{2+} or Zn^{2+} were not successful, MALDI-TOF mass spectroscopic measurements on the mixtures of PN_8 with the two metal ions could provide valuable information on the complex structures [13]. Typically, as for the mixture of PN_8 and Cu^{2+}, a strong peak at *m/z* of 1172.93 was observed, which was corresponding to the *m/z* of $[1[PN_8]+Cu^{2+}-H^+]^+$, thus suggesting the prevailing of the species in the form of 1:1 binding mode (Fig. S6 in Supporting information). Furthermore, the binding stoichiometry between PN_8 and the ions was explored *via* UV–vis spectroscopic titration with a fixed concentration of 0.1 mmol/L [28]. A peak in the obtained Job plot at the molar fraction of 0.5 was found (Fig. 4c), again confirming the 1:1 (or n:n) binding stoichiometry. In addition, according to the ^1H NMR spectra, the proton signals of the PN_8 and Cu^{2+} mixture disappeared (for aromatic protons) or became less-resolved (for alkyl protons), which suggested a shielding effect very likely caused by supramolecular interactions between PN_8 and Cu^{2+} (Fig. 4d). Similar results were found for Zn^{2+}, except for the possible co-existence of two complexes ($[1[PN_8]+Zn^{2+}-H^+]^+$ and $[2[PN_8]+Zn^{2+}-H^+]^+$), since there were two peaks at *m/z* of 1173.22 and 2288.70 according to MALDI-TOF mass spectroscopy (Fig. S7 in Supporting information). Taken together, these characterizations jointly manifested the good selectivity and sensitivity of the ion-sensing/binding properties of PN_8 towards Cu^{2+} and Zn^{2+}, in colorimetric and fluorometric modes.

Since PN_8 was not soluble in water and showed excellent and reversible metal ions binding ability in solution, its application as a solid-state adsorbent to remove Cu^{2+} and Zn^{2+} from aqueous solutions was examined. For demonstration, a small-size column with PN_8 powder as the filler, methanol and water as the eluent was fabricated. As shown in Fig. 5a, the pristine powder was yellow and emitted bright yellow fluorescence. Then, after the aqueous solutions of Cu^{2+} or Zn^{2+} were poured into the column, the successful adsorption of Cu^{2+} and Zn^{2+} could be observed with the color of the column changed to brown and orange, respectively. And under UV light, the corresponding column exhibited either quenched emission or orange fluorescence. All these changes were consistent with those in the solution. At the same time, the metal ion concentration before and after filtration was measured by ICP-MS (Fig. 5b) [29], which confirmed that a small amount of PN_8 (10 mg) could remove most of the Cu^{2+} and Zn^{2+} from the respective aqueous solution (1×10^{-4} mol/L, 4 mL). The removal efficiency was estimated to be 54.27% and 44.30% for Cu^{2+} and Zn^{2+}, respectively,

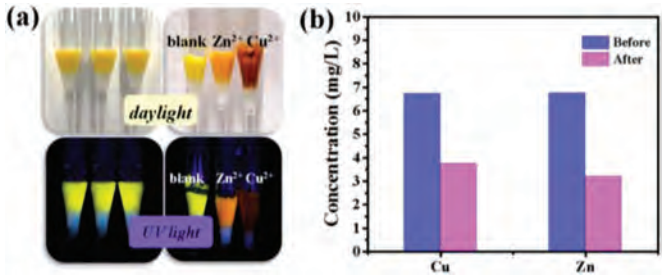

Fig. 5. (a) Photographs of glass pipettes filled with PN_8 powders under daylight and UV light before and after adsorption of Cu^{2+} and Zn^{2+} (1×10^{-3} mol/L). (b) The ion concentrations before and after the aqueous solutions were filtrated.

indicating good absorptivity of PN_8 (Fig. S8 in Supporting information). Notably, benefiting greatly from its large PAH core, PN_8 was highly hydrophobic and stable. So compared to other HAT-based materials, PN_8 is more suitable to be utilized as an optical ion probe and adsorbent, particularly in solid state, with the merits of high (fluorescence) color contrast, good stability and recyclability [30–35].

In conclusion, we have successfully synthesized a new HAT based, large PAH disc molecule (PN_8). PN_8 exhibited fluorescent sensing characteristics, which was selective for Cu^{2+} and Zn^{2+} over many other ions. The enlarged PAH core (up to 11 fused aromatic rings) and the doped hetero atoms endowed PN_8 good anisotropic self-assembly ability, metal-ion binding affinity and pronounced optical properties. Therefore, in self-assembled state, revisable morphological transition was found upon the alternate treatment of ions and EDTA. In solution state, the two ions triggered highly appreciable optical changes with high (fluorescence) color contrast and low detection limits, which were proved mainly based on the metal ion binding mode in different stoichiometric ratios. Importantly, due to its good stability and efficient ion binding capability, PN_8 was demonstrated as an excellent adsorbent to remove Cu^{2+} and Zn^{2+} from wastewater. The current work thus will not only enrich the family and the functions of heteroatom containing PAHs, but also be helpful for future applications of HAT-embedded disc molecules in advanced fluorescent sensing and imaging, water treatment and so on.

Declaration of competing interest

There are no conflicts to declare.

Acknowledgment

This work was supported by the National Key Research and Development Program of China (Nos. 2017YFA0204503 and 2017YFA0207800).

Supplementary materials

Supplementary material associated with this article can be found, in the online version, at doi:10.1016/j.cclet.2021.05.044.

References

[1] J.L. Segu, J. Segura, R. Juárez, M. Ramos, C. Seoane, Chem. Soc. Rev. 44 (2015) 6850–6885.
[2] Z.Y. Xiao, X. Zhao, X.K. Jiang, Z.T. Li, Chem. Mater. 23 (2011) 1505–1511.
[3] M. Han, G.C. Wang, H.Q. Duan, Chin. Chem. Lett. 25 (2014) 51–54.
[4] G.R. Kiel, M.S. Ziegler, T.D. Tilley, Angew. Chem. Int. Ed. 56 (2017) 4839–4844.
[5] Y. Dorca, C. Naranjo, P. Delgado-Martínez, R. Gómez, L. Sánchez, Chem. Commun. 55 (2019) 6070–6073.
[6] M. Wang, Y. Li, H. Tong, et al., Org. Lett. 13 (2011) 4378–4381.
[7] Y. Li, M.G. Li, Y.J. Su, et al., Chin. Chem. Lett. 27 (2016) 475–480.
[8] J. Ma, K. Zhang, K.S. Schellhammer, et al., Chem. Sci. 10 (2019) 4025–4031.
[9] Z.G. Tao, X. Zhao, X.K. Jiang, Z.T. Li, Tetrahedron Lett. 53 (2012) 1840–1842.
[10] W. Yuan, J. Cheng, X. Li, et al., Angew. Chem. Int. Ed. 59 (2020) 9940–9945.
[11] X.Y. Yan, M.D. Lin, S.T. Zheng, et al., Tetrahedron Lett. 59 (2018) 592–604.
[12] A. Yadav, D.K. Panda, S. Zhang, W. Zhou, S. Saha, ACS Appl. Mater. Interfaces 12 (2020) 40613–40619.
[13] X. Zhang, J. Fu, T.G. Zhan, et al., Tetrahedron Lett. 55 (2014) 6486–6489.
[14] S. Ibáñez, M. Poyatos, E. Peris, Chem. Commun. 53 (2017) 3733–3736.
[15] T.S. Saeed, D. Maddipatla, B.B. Narakathu, et al., RSC Adv. 9 (2019) 39824–39833.
[16] R. Juárez, M.M. Oliva, M. Ramos, et al., Chem. Eur. J. 17 (2011) 10312–10322.
[17] Z.G. Tao, T.G. Zhan, T.Y. Zhou, X. Zhao, Z.T. Li, Chin. Chem. Lett. 24 (2013) 453–456.
[18] T. Wang, H. Wang, G. Li, et al., Macromolecules 49 (2016) 4088–4094.
[19] W. Yuan, X. Ren, M. Li, et al., Angew. Chem. Int. Ed. 130 (2018) 6269–6273.
[20] J. Mei, N.L. Leung, R.T. Kwok, J.W. Lam, B.Z. Tang, Chem. Rev. 115 (2015) 11718–11940.
[21] J.K. Salunke, F.L. Wong, K. Feron, et al., J. Mater. Chem. C 4 (2016) 1009–1018.
[22] T. Ishi-i, R. Hirashima, N. Tsutsumi, et al., J. Org. Chem. 75 (2010) 6858–6868.
[23] M. Tanaka, T. Ikeda, J. Mack, N. Kobayashi, T. Haino, J. Org. Chem. 76 (2011) 5082–5091.
[24] Y. Han, W. Yuan, H. Wang, et al., J. Mater. Chem. C 6 (2018) 10456–10463.
[25] X.H. Zhang, Q. Zhao, X.M. Liu, et al., Talanta 108 (2013) 150–156.
[26] Z. Liu, C. Peng, Y. Wang, M. Pei, G. Zhang, Org. Biomol. Chem. 14 (2016) 4260–4266.
[27] L.C. da Silva, V.G. Machado, F.G. Menezes, Chem. Paper. 75 (2021) 1775–1793.
[28] T. Tian, T. Qian, T. Jiang, et al., Chem. Commun. 56 (2020) 3939–3942.
[29] D. Kou, W. Ma, S. Zhang, Adv. Funct. Mater. 31 (2021) 2007032.
[30] R. Juárez, M. Ramos, J. Segura, et al., J. Org. Chem. 75 (2010) 7542–7549.
[31] X.H. Zhang, C.F. Zhao, Y. Li, et al., Talanta 119 (2014) 632–638.
[32] J.O. Moilanen, B.M. Day, T. Pugh, R.A. Layfield, Chem. Commun. 51 (2015) 11478–11481.
[33] J.O. Moilanen, N.F. Chilton, B.M. Day, T. Pugh, R.A. Layfield, Angew. Chem. Int. Ed. 55 (2016) 5521–5525.
[34] V.J. Bhanvadia, A.L. Patel, S.S. Zade, N. J. Chem. 42 (2018) 17700–17707.
[35] A. Markovic, L. Gerhards, P. Sander, et al., ChemPhysChem 21 (2020) 2506–2514.